/

Article / Book Information

Title	Spin Oscillations in Antiferromagnetic NiO Triggered by Circularly Polarized Light
Authors	Takuya Satoh, Sung-Jin Cho, Ryugo Iida, Tsutomu Shimura, Kazuo Kuroda, Hiroaki Ueda, Yutaka Ueda, Boris A. Ivanov, Franco Nori, Manfred Fiebig
Citation	Physical Review Letters, Vol. 105, Issue 7, pp. 077402-1-4
Pub. date	2010, 8
Pub. version	http://dx.doi.org/10.1103/PhysRevLett.105.077402
Copyright	(C) 2010 American Physical Society

Spin Oscillations in Antiferromagnetic NiO Triggered by Circularly Polarized Light

Takuya Satoh,[1] Sung-Jin Cho,[1] Ryugo Iida,[1] Tsutomu Shimura,[1] Kazuo Kuroda,[1] Hiroaki Ueda,[2] Yutaka Ueda,[2]
B. A. Ivanov,[3,4] Franco Nori,[4,5] and Manfred Fiebig[6]

[1]*Institute of Industrial Science, University of Tokyo, Tokyo 153-8505, Japan*
[2]*Institute for Solid State Physics, University of Tokyo, Kashiwa, Chiba 277-8581, Japan*
[3]*Institute of Magnetism, Vernadskii Avenue 36B, 03142 Kiev, Ukraine*
[4]*RIKEN Advanced Science Institute, Wako-shi, Saitama, 351-0198, Japan*
[5]*Department of Physics, University of Michigan, Ann Arbor, Michigan 48109-1040, USA*
[6]*HISKP, Universität Bonn, Nussallee 14-16, 53115 Bonn, Germany*
(Received 2 December 2009; published 11 August 2010)

Coherent spin oscillations were nonthermally induced by circularly polarized pulses in the fully compensated antiferromagnet NiO. This effect is attributed to the action of the effective magnetic field generated by an inverse Faraday effect on the spins. The novelty of this mechanism is that spin oscillations are driven by the time derivative of the effective magnetic field which acts even on "pure" antiferromagnets with zero net magnetic moment in the ground state. The measured frequencies (1.07 THz and 140 GHz) correspond to the out-of-plane and in-plane modes of antiferromagnetic spin oscillations.

All-optical magnetization switching has been extensively studied in recent years. Demagnetization within 1 ps was discovered by irradiating ferromagnetic nickel with femtosecond laser pulses [1]. This finding has stimulated intense theoretical and experimental investigations. Many of the experiments on so-called "ultrafast magnetism" can be interpreted in terms of laser-induced heating, which is already exploited technologically in the form of heat-assisted magnetic recording [2]. However, the recording rate is limited by slow thermal diffusion. Thus, magnetization control beyond the limit of such thermal control is highly desirable.

A typical form of nonthermal magnetization control is the inverse Faraday effect (IFE) [3,4] in which circularly polarized light induces a magnetization that can be described as a light-induced effective magnetic field acting on the body. A pump-probe technique with subpicosecond time resolution has revealed a transient IFE at zero time delay in itinerant ferromagnets [5–8]. However, the validity was questioned because the observation was restricted to the temporal overlap of the pump and probe pulses [9].

The dynamic properties of antiferromagnets (AFMs) are rapidly gaining importance [10,11]. They display inherently faster spin dynamics than ferromagnets [10–12] and offer the advantage that the spin oscillation frequency extends into the terahertz regime. In addition, ultrafast manipulation of the antiferromagnetic order parameter may be employed for ultrafast control of the magnetization of an adjacent ferromagnet via the exchange-bias effect. Recently, spin precession caused by the IFE has been reported for ferrite garnets [13] and for canted AFMs [11,14], which possess nonzero net magnetic moment caused by the Dzyaloshinskii-Moriya interaction. The presence of this magnetic moment is an important issue for the recently proposed mechanism of inertia-driven

excitation of spin oscillations in canted AFMs [15]. However, fully nonthermal control of spin oscillations has not been demonstrated yet in "pure" AFMs, having a compensated magnetic moment ($\vec{M} = 0$) in the ground state.

Here we report the first observation of coherent spin oscillations in the compensated AFM NiO in a pump-probe experiment. The oscillations consisted of 1.07 THz and 140 GHz components, which are assigned to out-of-plane and in-plane modes of antiferromagnetic spin oscillations. The sign of the oscillation was reversed with the reversal of the pump helicity. This is interpreted within the σ model as a direct action of the *time derivative* of the impulsive magnetic field generated by a circularly polarized pulse via the IFE on the zero-magnetization AFM. This mechanism (discussed in Refs. [16,17] but never observed before) opens a novel way for the ultrafast control of spins in compensated AFMs.

NiO is a promising exchange-bias AFM because of its simple structure and room-temperature antiferromagnetism. Therefore, the investigation of the time-resolved responses of NiO is important for applications of ultrafast optical switching and in fundamental research. The subpicosecond spin reorientation in NiO has been achieved by modifying the magnetocrystalline anisotropy with linearly polarized light [18]. However, this process depends on a resonant optical excitation and is thus limited by thermal effects.

Above the Néel temperature ($T_N = 523$ K), NiO has a NaCl-type cubic structure (point group: $m\bar{3}m$). Below T_N, NiO has antiferromagnetic order. The Ni^{2+} spins align ferromagnetically along the $\langle 11\bar{2}\rangle$ axes in $\{111\}$ planes with antiferromagnetic coupling in between adjacent $\{111\}$ planes [19]. Exchange striction leads to a contraction of the cubic unit cell along the $\langle 111 \rangle$ axes and reduces the crystallographic symmetry to $\bar{3}m$. This gives rise to four

types of twin (T) domains. The deformation is accompanied by magnetic birefringence between the {111} plane and the ⟨111⟩ direction. NiO is a charge-transfer insulator with a 4 eV band gap. The intragap optical transition in the midinfrared to visible region is ascribed to the d-d transitions of the $Ni^{2+}(3d^8)$ electrons [20].

A NiO single crystal grown by the floating-zone method was polished into (111)-oriented platelets with lateral dimensions of a few millimeters and a thickness of ≃100 μm. To obtain T domains of 0.1–1 mm, the platelets were annealed in an argon-oxygen mixture with small oxygen partial pressure at 1400 °C [21]. Four types of T domains were distinguished in the cross-Nicol configuration [22]. For the pump-probe measurement, we selected a single T domain with the ($1\bar{1}1$) plane different from the sample surface (111), as shown in Fig. 1(a).

The temporal evolution of the polarization rotation and transmission was measured at 77 K with a pump-probe setup with no external magnetic field [Fig. 1(b)]. Linearly polarized light from a Ti:sapphire laser with a wavelength of 792 nm, a pulse width of 120 fs, and a repetition rate of 1 kHz was used as the probe. Circularly polarized optical pulses with a wavelength of 1280 nm, generated by an optical parametric amplifier, were used as the pump. The pump and probe beams were incident at 7° and 0°, respectively, and focused onto the sample surface to spot sizes of about 100 and 40 μm, respectively. The pump fluence was 10 mJ/cm², which corresponds to the absorption of about one photon per 10^4 Ni^{2+} ions. The transmitted probe beam was divided into two orthogonally polarized components
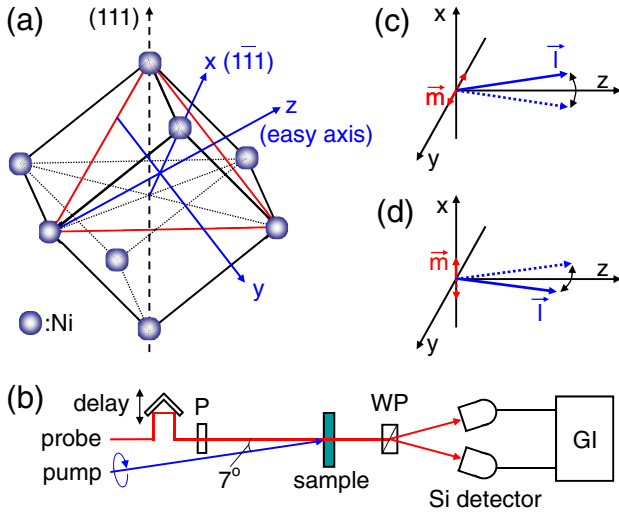
for obtaining the polarization rotation and the transmission change.

To clarify the spin-related contribution, we examined the response after photoexcitation with different time delays. Figures 2(a) and 2(b) show the polarization rotation and the transmission change, respectively, versus the time delay between the probe beam and the pump beam. The inset in Fig. 2 shows the polarization rotation of the probe beam near zero delay. Here the signal is compared for $\sigma(+)$ and $\sigma(-)$ polarized pump beams at fixed laser fluence. In Fig. 2, two processes can be distinguished: (1) a fast (quasi-instantaneous) change of the polarization rotation within the time of the pulse action (inset) and (2) damped oscillations of the polarization rotation which persists for much longer times (upper frame).

In regime (1), for short time delays (≲1 ps), the rotation exceeded 20 mrad when the pump and the probe beams overlapped temporally. The full width at half maximum of the signal was about 200 fs, which reflects the duration of the pump and probe pulses. In regime (2), damped oscillations of the signal were observed at times longer than 10 ps. For both time intervals, the sign of the signal changes with reversal of the pump helicity, which is a clear indication of the nonthermal origin of the effect. Note the significant difference in the amplitude of the rotation angle observed at these two time scales (≲0.2 and ≳1 ps) that

FIG. 1 (color online). (a) Geometry of the experiment. The (111) direction coincides with the normal to the sample; the ($1\bar{1}1$) direction (x axis), y axis, and z axis, respectively, are the hard, medium, and easy axes for the T domain of our measurement (red triangle). (b) Schematic diagram of the experimental setup. (P: polarizer; WP: Wollaston prism; GI: gated integrator). (c),(d) Schematics of the oscillations of vectors $\vec{l}$ and $\vec{m}$ (blue and red arrows, respectively) for the out-of-plane and in-plane modes of the spin oscillations.
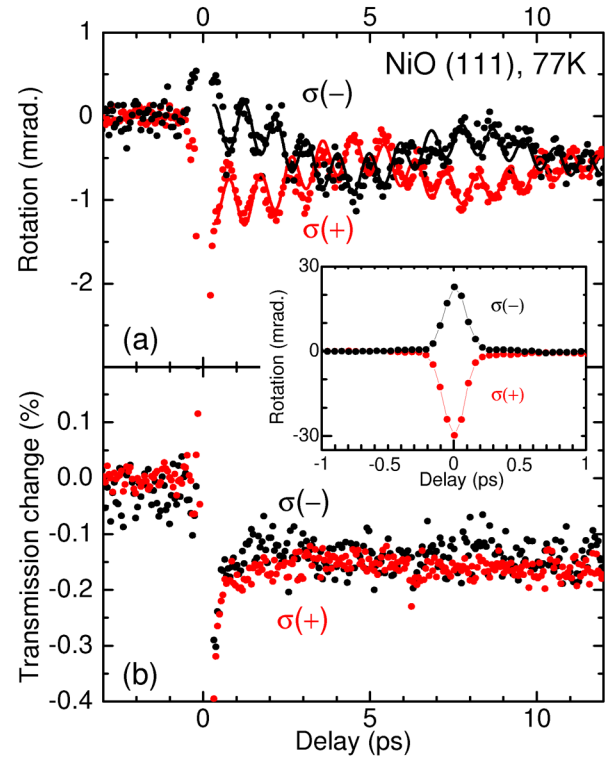

FIG. 2 (color online). Time-resolved (a) polarization rotation and (b) transmission change in NiO (111) for pump helicities $\sigma(+, -)$. Pump wavelength: $\lambda_e = 1280$ nm; probe wavelength: $\lambda_p = 792$ nm.

likely reflects the difference of the mechanisms responsible for them.

Process (1) can be considered as a typical example of *femtomagnetism*, arising at times much shorter than the thermalization time [23]. A description of this regime involves either a direct transfer of photon angular momentum to the medium or a photoenhanced transfer between orbital and spin momenta [8,13,23–25]. For NiO, the orbital momentum of the ground state $(^3\Gamma_2)$ of the $Ni^{2+}(3d^8)$ ion is quenched due to orbital nondegeneracy. In the virtually excited state, the orbital momentum is ± 1 depending on the helicity $\sigma(\pm)$ of the pump beam, which leads to the appearance of a transient magnetization. Recently, *ab initio* calculations [26] of an ultrafast laser-induced spin switch in NiO has demonstrated the possibility of inducing a spin magnetic moment at <100 fs that results in *instantaneous* magneto-optical effects.

In process (2), the sign of the oscillations in the polarization rotation changes with reversal of the pump helicity. No oscillation is observed in the transmission, indicating that the oscillation in the rotation is magnetic in origin. The damped oscillations are fitted by $\sum_{i=1,2} a_i \cos(2\pi f_i t + \phi_i)\exp(-t/\tau_i)$. The data in Fig. 2(a) yield $a_1 = 0.3$ mrad, $f_1 = 1.07$ THz, $\phi_1 = 1.0$, $\tau_1 = 15$ ps, $a_2 = 0.375$ mrad, $f_2 = 140$ GHz, $\phi_2 = 2.2$, and $\tau_2 = 10$ ps. This behavior is not sinelike, as for canted AFMs [15]. A small deviation from the cosinelike behavior [17] (see below) can be attributed to surface effects (like for optical phonons [27]).

At these time scales some magnon modes are excited in the spin system. The coherent spin oscillations modulate the dielectric permittivity, leading to a rotation of the probe polarization (see below). Since the net magnetization is zero in the ground state, the mechanism inducing spin oscillations is different from that in ferrimagnets or in canted AFMs. Such excitation in NiO cannot be attributed to the mechanism discussed in Ref. [15], for which the presence of *nonzero* net magnetic moment in the ground state is necessary. Instead, the dynamics of pure AFMs can be described by the σ model with the derivative $d\vec{H}(t)/dt$ as a driving force [17]. Let us now discuss process (2) within the σ model.

For the theoretical description of the spin excitations, we employ a model of NiO with two sublattices with magnetizations $\vec{M}_1$ and $\vec{M}_2$, $|\vec{M}_1| = |\vec{M}_2| = M_0$, coupled by the antiferromagnetic next-nearest neighbor exchange interaction J [19]. For such AFMs, the antiferromagnetic vector $\vec{L} = \vec{M}_1 - \vec{M}_2$ is the principal dynamical variable. Within the σ model, the equation for the normalized (unit) vector $\vec{l} = \vec{L}/|\vec{L}|$ can be written through the variation of the Lagrangian $\mathcal{L}[\vec{l}]$ (see [16,28]):

$$\mathcal{L} = \frac{\hbar}{2\gamma H_{ex}}\left(\frac{\partial\vec{l}}{\partial t}\right)^2 - \mathcal{W}(\vec{l}) - \frac{\hbar}{H_{ex}}\left[\vec{H}\cdot\left(\vec{l}\times\frac{\partial\vec{l}}{\partial t}\right)\right]. \quad (1)$$

Here the first two terms describe the free oscillations of the

spins, and the last term determines the action of the circularly polarized light described by an effective magnetic field $\vec{H}(t) \propto (\vec{E}\times\vec{E}^*)$, corresponding to the IFE. The value of the Lagrangian is presented per one spin. We have $\gamma = g\mu_B/\hbar$ as the gyromagnetic ratio, g as the Landé factor, μ_B as the Bohr magneton, $H_{ex} = zSJ/g\mu_B$ as the exchange field of AFM, and $z = 6$ as the number of next-nearest neighbors. For NiO, $J = 221$ K, which for $S = 1$ gives $\gamma H_{ex} = zSJ/\hbar = 27.4$ THz. We used the simplest form of the biaxial anisotropy $\mathcal{W}(\vec{l}) = g\mu_B(H_{a1}l_x^2 + H_{a2}l_y^2)$, written in terms of the out-of-plane anisotropy field H_{a1} and much smaller in-plane anisotropy field H_{a2} [19]. Within the σ model, the magnetization $\vec{M} = \vec{M}_1 + \vec{M}_2 = 2M_0\vec{m}$ is a slave variable and can be written as [16,28]

$$H_{ex}\vec{m} = [\vec{H} - \vec{l}(\vec{H}\cdot\vec{l})] + \frac{1}{\gamma}\left(\frac{\partial\vec{l}}{\partial t}\times\vec{l}\right), \quad (2)$$

where the first term determines the canting of the sublattices, caused by the effective magnetic field $\vec{H}$, and the second term describes the dynamic contribution.

The variation of $\mathcal{L}[\vec{l}]$ gives the dynamical equations for $\vec{l}$. In linear approximation over the deviation from the ground state ($\vec{l}_{ground} \parallel z$; see Fig. 1), they read

$$\frac{\partial^2 l_x}{\partial t^2} + \omega_1^2 l_x = \gamma\frac{dH_y}{dt}; \frac{\partial^2 l_y}{\partial t^2} + \omega_2^2 l_y = -\gamma\frac{dH_x}{dt}, \quad (3)$$

where $\omega_1 = \gamma\sqrt{2H_{ex}H_{a1}}$ and $\omega_2 = \gamma\sqrt{2H_{ex}H_{a2}}$ are the frequencies of the out-of-plane and in-plane antiferromagnetic spin oscillations, respectively, omitting the dissipation terms. For a short pulse ($\omega_{1,2}\Delta t \ll 1$), Eq. (3) describes a universal behavior for AFMs [17]. Namely, after the pulse action, for $t \gg \Delta t$, the spins exhibit free oscillations with frequencies $\omega_{1,2}$ and amplitudes $l_x(t = 0) = \gamma\bar{H}_y\Delta t$ and $l_y(t = 0) = -\gamma\bar{H}_x\Delta t$, where $\bar{H}_{x,y}\Delta t \equiv \int_{-\infty}^{+\infty} H_{x,y}(t)dt$, determined by the form of the pulse. Thus, the amplitudes are determined by the total fluence connected to the pulse field components, H_y and H_x, and these amplitudes are not dependent on the pulse shape or duration (for our case, $\omega\Delta t \ll 1$). This situation is also common for the inertial mechanism for canted AFMs [15]. However, for canted AFMs the pulse produces an initial "spin speed" $d\phi/dt|_{t=+0}$, and for pure AFMs, the "initial spin deviation" is $\phi|_{t=+0}$, where ϕ is an angular variable for $\vec{l}$. For this reason, cosinelike oscillations appear in Fig. 2(a) (instead of sinelike, for the canted AFMs investigated before). The oscillation of the vector $\vec{m}$ produces a modulation of the antisymmetric part of the permittivity tensor ε_{ij}, $\Delta\varepsilon_{ij}^a \propto e_{ijk}m_k$, where e_{ijk} is the totally antisymmetric tensor. In linear approximation, the out-of-plane mode produces $\Delta\varepsilon_{xz}^a \propto m_y$, and the in-plane mode produces $\Delta\varepsilon_{yz}^a \propto m_x$.

For our measurements, a T domain inclined to the surface of the sample was chosen [see Fig. 1(a)], and the values of H_y and H_x were approximately equal, in agree-

ment with the observation that $a_1 \sim a_2$. The measured frequency $f_1 = 1.07$ THz is in good agreement with the out-of-plane mode of the antiferromagnetic spin oscillations. From the out-of-plane anisotropy, $\gamma H_{a1} \simeq 23$ GHz [19], one obtains $f_1 = 1.1$ THz. The 1.07 THz component has been observed in far-infrared antiferromagnetic resonance [29,30] and Raman scattering [31]. The small in-plane anisotropy field $\gamma H_{a2} \sim 1$ GHz is not well known [19], but spin oscillations with a frequency $f_2 = 140$ GHz have recently been observed in NiO by Brillouin scattering [32]. This strongly suggests that the oscillations in Fig. 2(a) at ≥ 1 ps are spin oscillations around the easy axis, which are the usual spin-wave modes, triggered by the effective magnetic field $\vec{H}$ generated via the IFE, with the time derivative of the field $d\vec{H}/dt$ working as a torque acting on the vector $\vec{l}$.

The simultaneous observation of the magnetic response at both short times and long times, in processes (1) and (2), allows us to reach conclusions about the applicability of different approaches to describe the spin dynamics. The Landau-Lifshitz equation for ferromagnets (or, equivalently, the σ-model equation for AFMs) describes the dynamics of spin systems in terms of only the magnetization vector (or sublattice magnetizations, for AFMs). These equations are valid for quasiequilibrium states, where these magnetizations are formed by the exchange interaction. This occurs (according to our observations) for times corresponding to process (2). On the other hand, our results show that the σ-model approach (like other theories treating the dynamics of spin systems through the mean value of the magnetization) is not sufficient to describe shorter times $t \lesssim 0.5$ ps, namely, the behavior in regime (1). For instance, the amplitudes of the oscillation $l_{x,y}(0)$ do not contain anisotropy fields, and they can be obtained by neglecting all relativistic interactions in the AFM, except for the Zeeman interaction of the spins with the pulsed magnetic field. In this approximation within the σ-model approach, the projection of the magnetization parallel to the field is conserved and cannot appear during the action of a short ($\Delta t \ll 1/\omega_{1,2}$) field pulse. For the σ model, direct calculations show that the static and dynamic contributions to the magnetization [Eq. (2)] compensate each other in this short time interval [17]. On the other hand, the signal observed at these times is much higher than for process (2). Thus, to describe the initial stage (1), one needs to use a more detailed analysis involving the spin and orbital momenta of the solid and the angular momentum of photons [26].

In conclusion, the time-resolved magneto-optical response of NiO provides direct access to the magnetization changes under the action of laser pulse irradiation. We found that compensated antiferromagnetic NiO shows spin oscillations triggered nonthermally by a circularly polarized pulse, with the time derivative $d\vec{H}/dt$ as the driving force acting on the antiferromagnetic vector $\vec{l}$. The 1.07 THz and 140 GHz components are in good agreement with reported values for antiferromagnetic spin oscillations. We thus extend the potential of NiO as an antiferromagnetic constituent in spintronic devices, from static and thermally limited spin-dynamical experiments into the range of all-optical magnetization control at terahertz frequencies.

[1] E. Beaurepaire *et al.*, Phys. Rev. Lett. **76**, 4250 (1996).
[2] L. Pan and D. B. Bogy, Nat. Photon. **3**, 189 (2009).
[3] L. P. Pitaevskii, Sov. Phys. JETP **12**, 1008 (1961).
[4] J. P. van der Ziel *et al.*, Phys. Rev. Lett. **15**, 190 (1965).
[5] G. Ju *et al.*, Phys. Rev. B **57**, R700 (1998).
[6] P. J. Bennett *et al.*, Opt. Lett. **24**, 1373 (1999).
[7] R. Wilks *et al.*, J. Phys. Condens. Matter **15**, 5129 (2003).
[8] F. Dalla Longa *et al.*, Phys. Rev. B **75**, 224431 (2007).
[9] B. Koopmans *et al.*, Phys. Rev. Lett. **85**, 844 (2000).
[10] A. V. Kimel *et al.*, Nature (London) **429**, 850 (2004).
[11] A. V. Kimel *et al.*, Nature (London) **435**, 655 (2005).
[12] T. Satoh *et al.*, Phys. Rev. B **75**, 155406 (2007).
[13] F. Hansteen *et al.*, Phys. Rev. B **73**, 014421 (2006).
[14] A. M. Kalashnikova *et al.*, Phys. Rev. Lett. **99**, 167205 (2007).
[15] A. V. Kimel *et al.*, Nature Phys. **5**, 727 (2009).
[16] A. F. Andreev and V. I. Marchenko, Sov. Phys. Usp. **23**, 21 (1980).
[17] A. Yu. Galkin and B. A. Ivanov, JETP Lett. **88**, 249 (2008).
[18] N. P. Duong *et al.*, Phys. Rev. Lett. **93**, 117402 (2004).
[19] M. T. Hutchings and E. J. Samuelsen, Phys. Rev. B **6**, 3447 (1972).
[20] M. Fiebig *et al.*, Phys. Rev. Lett. **87**, 137202 (2001).
[21] I. Sänger *et al.*, Phys. Rev. B **74**, 144401 (2006).
[22] T. Satoh *et al.*, J. Opt. Soc. Am. B **27**, 1421 (2010).
[23] J.-Y. Bigot *et al.*, Nature Phys. **5**, 515 (2009).
[24] G. P. Zhang and T. F. George, Phys. Rev. B **78**, 052407 (2008).
[25] M. I. Kurkin *et al.*, Phys. Rev. B **78**, 134430 (2008).
[26] G. Lefkidis *et al.*, Phys. Rev. Lett. **103**, 217401 (2009).
[27] Y. Liu *et al.*, Phys. Rev. Lett. **75**, 334 (1995).
[28] V. G. Baryakhtar *et al.*, *Dynamics of Topological Magnetic Solitons. Experiment and Theory*, Springer Tracts in Modern Physics Vol. 139 (Springer, Berlin, 1994); V. G. Baryakhtar, B. A. Ivanov, and M. V. Chetkin, Sov. Phys. Usp. **28**, 563 (1985).
[29] H. Kondoh, J. Phys. Soc. Jpn. **15**, 1970 (1960).
[30] A. J. Sievers III and M. Tinkham, Phys. Rev. **129**, 1566 (1963).
[31] D. J. Lockwood, M. G. Cottam, and J. H. Baskey, J. Magn. Magn. Mater. **104–107**, 1053 (1992).
[32] J. Milano *et al.*, Phys. Rev. Lett. **93**, 077601 (2004).